

Article

# Alginate NiFe<sub>2</sub>O<sub>4</sub> Nanoparticles Cryogel for Electrochemical Glucose Biosensor Development

Amin Fatoni <sup>1,\*</sup> , Aziz Wijonarko <sup>1</sup>, Mekar Dwi Anggraeni <sup>2</sup>, Dadan Hermawan <sup>1</sup>, Hartiwi Diastuti <sup>1</sup> and Zusfahair <sup>1</sup>

<sup>1</sup> Department of Chemistry, Faculty of Mathematics and Natural Sciences, Universitas Jenderal Soedirman, Purwokerto 53122, Indonesia; wijonarkoaziz@gmail.com (A.W.); dadan.hermawan@unsoed.ac.id (D.H.); hartiwi.diastuti@unsoed.ac.id (H.D.); zusfahair@unsoed.ac.id (Z.)

<sup>2</sup> Department of Nursing, Faculty of Health Sciences, Universitas Jenderal Soedirman, Purwokerto 53122, Indonesia; mekar.anggraeni@unsoed.ac.id

\* Correspondence: aminfatoni@unsoed.ac.id

**Abstract:** Glucose biosensors based on porous material of alginate cryogel has been developed, and the cryogel provides a large surface area for enzyme immobilization. The alginate cryogel has been supplemented with NiFe<sub>2</sub>O<sub>4</sub> nanoparticles to improve the electron transfer for electrochemical detection. The fabrication parameters and operational conditions for the biosensor have also been optimized. The results showed that the optimum addition of NiFe<sub>2</sub>O<sub>4</sub> nanoparticles to the alginate solution was 0.03 g/mL. The optimum operational conditions for the electrochemical detection were a cyclic voltammetry scan rate of 0.11 V/s, buffer pH of 7.0, and buffer concentration of 150 mM. The fabricated alginate NiFe<sub>2</sub>O<sub>4</sub> nanoparticles cryogel-based glucose biosensor showed a linear response for glucose determination with a regression line of  $y = 18.18x + 455.28$  and  $R^2 = 0.98$ . Furthermore, the calculated detection limit was 0.32 mM and the limit of quantification was 1.06 mM.

**Keywords:** alginate; cryogel; electrochemical; glucose biosensor; nickel ferrite nanoparticles



**Citation:** Fatoni, A.; Wijonarko, A.; Anggraeni, M.D.; Hermawan, D.; Diastuti, H.; Zusfahair. Alginate NiFe<sub>2</sub>O<sub>4</sub> Nanoparticles Cryogel for Electrochemical Glucose Biosensor Development. *Gels* **2021**, *7*, 272. <https://doi.org/10.3390/gels7040272>

Academic Editors: Pavel Gurikov and Dmitry A. Berillo

Received: 23 October 2021

Accepted: 14 December 2021

Published: 17 December 2021

**Publisher's Note:** MDPI stays neutral with regard to jurisdictional claims in published maps and institutional affiliations.



**Copyright:** © 2021 by the authors. Licensee MDPI, Basel, Switzerland. This article is an open access article distributed under the terms and conditions of the Creative Commons Attribution (CC BY) license (<https://creativecommons.org/licenses/by/4.0/>).

## 1. Introduction

Diabetes mellitus is a degenerative disease that causes many deaths. About 43% of the 3.7 million deaths from diabetes mellitus occur before age of 70 years and the percentage of these deaths is higher in developing countries [1]. According to the International Diabetes Federation (IDF), in 2017, the prevalence of diabetes mellitus in the world reached 424.9 million people and is expected to reach 628.6 million in 2045 [2]. Diabetes mellitus is also found as the most comorbidities among individuals died due to COVID-19, especially in Central Java Province, Indonesia, with 39.7% and followed by hypertension at 31.6% (Central Java 2020).

There are preventive measures in place to reduce the number of people with diabetes mellitus. Previous strategies reported for early detection were to determine blood glucose levels with a biosensor [3]. In general, the glucose biosensor uses the enzyme glucose oxidase to catalyze the glucose conversion and the results could be detected electrochemically. The combination of biological sensing elements such as an enzyme and a transducer such as an electrochemical transducer is the main principle of the biosensor for analyte determination [4]. Biosensors have shown several advantages such as being easy to manufacture in small tools (portable), relatively inexpensive, high sensitivity, high selectivity, and making real-time measurements possible. As a result, they have been widely developed and commercialized as analytical tools [5].

The development of biosensors is generally focused on increasing their sensitivity, selectivity, stability, or reducing their production costs. The development strategies could be performed in the biological compound exploration of biological sensing elements such as enzymes, antibodies, cells, supporting materials for biological compound immobilization

or the detector improvisation. In developing an enzyme supporting material, a previous study showed that the use of chitosan cryogel increases the surface area of the electrode, thereby increasing the performance of electrochemical biosensors [6]. However, the non-conductive nature of chitosan reduces the electric current when it has been applied with an electrochemical transducer. Various strategies to improve the chitosan conductivity have been explored, such as using carbon nanotubes [7] and grafting with polyaniline [8]. However, it is still challenging to find better enzyme support materials for detecting glucose. Besides chitosan, another biopolymer showed an excellent property as porous supporting material is alginate. Alginate is hydrophilic, biocompatible and biodegradable [9]. Alginate has been used in tissue engineering [10], drug delivery [11], enzyme immobilization [12], and biosensors [13]. Furthermore, the calcium alginate matrix for enzyme immobilization could be easily prepared using a simple procedure compared to crosslinking of chitosan. The use of crosslinker agent such as glutaraldehyde is not environmentally friendly, and it could be cytotoxic in case of the biological sensing element using bacteria cell. The green technology using urea-induced gelation for chitosan crosslinking was a relatively complex procedure and resulted in non-stable gel compared to glutaraldehyde crosslinked [14]. Another advantage of alginate matrix compared to chitosan is that it has a greater capacity for biomolecule entrapment [15].

Despite the numerous advantages, the use of biomaterial such as chitosan and alginate in the application of biosensors with electrochemical detection has poor mechanical and electrical properties. It has been reported that composites made from biomaterials and nanoparticles overcome these poor electrical properties [7,16]. This research used nickel ferrite nanoparticles to improve the alginate cryogel for glucose biosensor application using electrochemical detection.

## 2. Results and Discussion

### 2.1. $\text{NiFe}_2\text{O}_4$ Nanoparticles Preparation and Characterization

The  $\text{NiFe}_2\text{O}_4$  nanoparticles were synthesized to improve the performance of the alginate cryogel modified electrode. The  $\text{NiFe}_2\text{O}_4$  nanoparticles were prepared using co-precipitation which was a bottom-up synthesis of nanoparticle from their metal ions to obtain nanosized particles. The co-precipitation method was selected because of its simplicity and ease of obtaining the homogenous size [17,18]. The obtained  $\text{NiFe}_2\text{O}_4$  nanoparticles were a brown powder (Figure 1A). The  $\text{NiFe}_2\text{O}_4$  nanoparticles prepared using the same procedure have been reported to have a particle size of 4.2–5.7 nm observed by transmission electron microscopy and magnetic coercivity of 42–47 Oe [19].

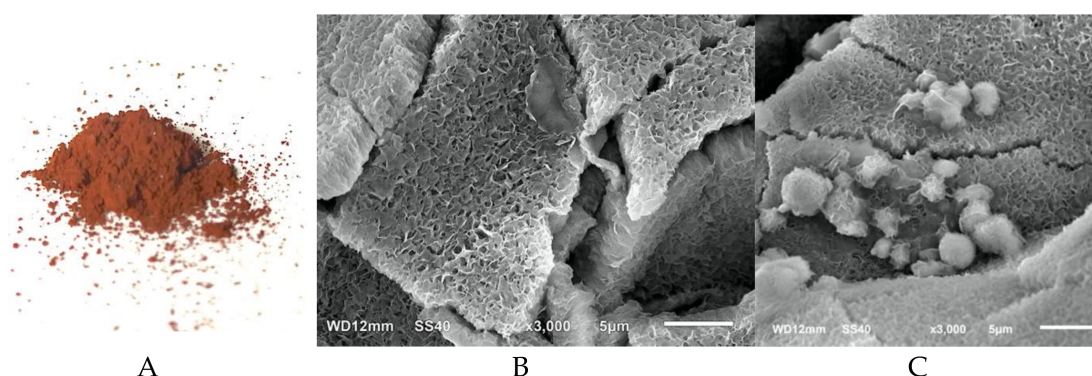


**Figure 1.** Synthesized  $\text{NiFe}_2\text{O}_4$  nanoparticles showed as a dark brown powder (A). The porous structure of cryogel is made of alginate (B) and alginate with  $\text{NiFe}_2\text{O}_4$  nanoparticles (C).

Alginate cryogel was formed by crosslinking sodium alginate under subzero temperature to freeze the water solvent and leave a porous structure [7]. The  $\text{NiFe}_2\text{O}_4$  nanoparticles were entrapped in the alginate structure to facilitate the electron transfer during the redox reaction of the working electrode. The scanning electron microscope image showed that

the porous alginate cryogel had a large surface area (Figure 1B,C) with a pore size of about 1–2 micron pores. Subsequently, the alginate NiFe<sub>2</sub>O<sub>4</sub> nanoparticles cryogel structure and alginate only cryogel showed a similar porous material with an aggregate of NiFe<sub>2</sub>O<sub>4</sub> nanoparticles on the surface of the alginate NiFe<sub>2</sub>O<sub>4</sub> nanoparticles cryogel.

## 2.2. Alginate NiFe<sub>2</sub>O<sub>4</sub> Nanoparticles Modified Electrode Performance

The performance of the alginate-NiFe<sub>2</sub>O<sub>4</sub> nanoparticles cryogel electrode was tested using potassium hexacyanoferrate and hydrogen peroxide. Potassium hexacyanoferrate was used to observe the electron transfer behavior of each step of electrode modification. The results showed that the glassy carbon electrode with alginate cryogel (Figure 2A, red) had lower oxidation and reduction peaks compared to a bare glassy carbon electrode (Figure 2A, blue). The lower oxidation and reduction peaks of alginate cryogel were due to the low conductivity characteristic of alginate [20]. Therefore, strategies to improve the alginate conductivity of the alginate are required. The alginate NiFe<sub>2</sub>O<sub>4</sub> nanoparticles cryogel showed higher oxidation and reduction peaks (Figure 2A, green), compared to both bare glassy carbon electrode and alginate cryogel modified electrode. The higher oxidation and reduction peaks of the NiFe<sub>2</sub>O<sub>4</sub> nanoparticles alginate cryogel due to the large surface area of porous cryogel combined with the nickel ferrite nanoparticles.

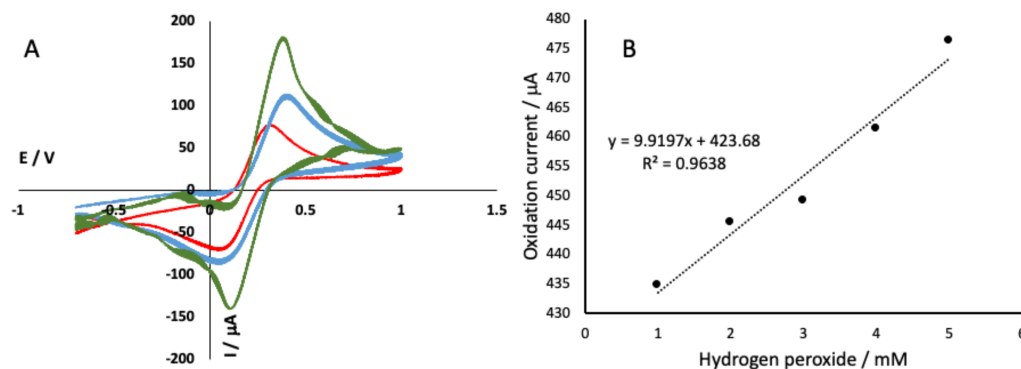


**Figure 2.** Electron transfer behavior of a bare glassy carbon electrode (A, blue line), alginate cryogel modified electrode (A, red line), and alginate-NiFe<sub>2</sub>O<sub>4</sub> nanoparticles cryogel modified electrode (A, green line) measured on 10 mM potassium ferricyanide. Alginate-NiFe<sub>2</sub>O<sub>4</sub> nanoparticles modified electrode showed a linear response for detecting hydrogen peroxide (B).

It was previously reported that nickel ferrite nanoparticles increase the conductivity of the compound with PANI [21], polypyrrole-chitosan [22] and alginic acid [23]. Besides improving the electron transfer of the alginate cryogel by adding NiFe<sub>2</sub>O<sub>4</sub> nanoparticles, this nanoparticle with the magnetic properties also makes the alginate cryogel become magnetic alginate cryogel. The magnetic alginate based gels have been reported in many fields such as biosensors [24], drug delivery [25] and tissue engineering [26]. The magnetic materials embedded in the gels provide unique features such as responding to the applied magnetic fields, inducing shape changes and modifying the mechanical properties [27]. The nanoparticle of NiFe<sub>2</sub>O<sub>4</sub> provides magnetism of small size ferromagnetic (superparamagnetism) showed unique properties that could enhance the biosensor sensitivity and allow rapid detection of various analytes [28]. Therefore, the increase of the redox peaks observed in this research can also be caused by the super magnetism of nanoparticles added to the alginate gels.

Hydrogen peroxide was first used to simulate the glucose biosensor, since the use of glucose oxidase enzyme would result in hydrogen peroxide which was eventually detected by electrochemical detection. The electrochemical method used was cyclic voltammetry, which is a cyclic method that describes the movement of electrons due to a reduction and oxidation reaction occurring on the surface of the working electrode. The results showed a linear response of hydrogen peroxide determination (1–5 mM, in phosphate buffer) using

alginate-NiFe<sub>2</sub>O<sub>4</sub> nanoparticles modified electrode performed using cyclic voltammetry (Figure 2B).

### 2.3. NiFe<sub>2</sub>O<sub>4</sub> Nanoparticles Addition Optimization

NiFe<sub>2</sub>O<sub>4</sub> nanoparticles were added to the alginate cryogel to improve the electron transfer properties. However, the addition of nanomaterials could be increasing the cost in further application. Therefore, finding the best condition with the lowest number of nanoparticles addition was important but showed the optimal electron transfer properties.

The NiFe<sub>2</sub>O<sub>4</sub> nanoparticles was added in various final concentration of 0.01, 0.02, 0.03, 0.04 and 0.05 g/mL of sodium alginate solution. The result showed the increase of oxidation current with the addition of NiFe<sub>2</sub>O<sub>4</sub> nanoparticles from 0.01 to 0.03 g/mL. However, the higher amount of the nanoparticles did not show a significant oxidation current change (Figure 3). The nanoparticle composite in alginate polymers was generally prepared in the composition of 0–10% (*w/v*) such as in the alginate-magnetic nanoparticles [29], alginate silver nanoparticles [30], alginate-Fe<sub>3</sub>O<sub>4</sub> nanoparticles [31] and alginate multi-walled carbon nanotubes [32].

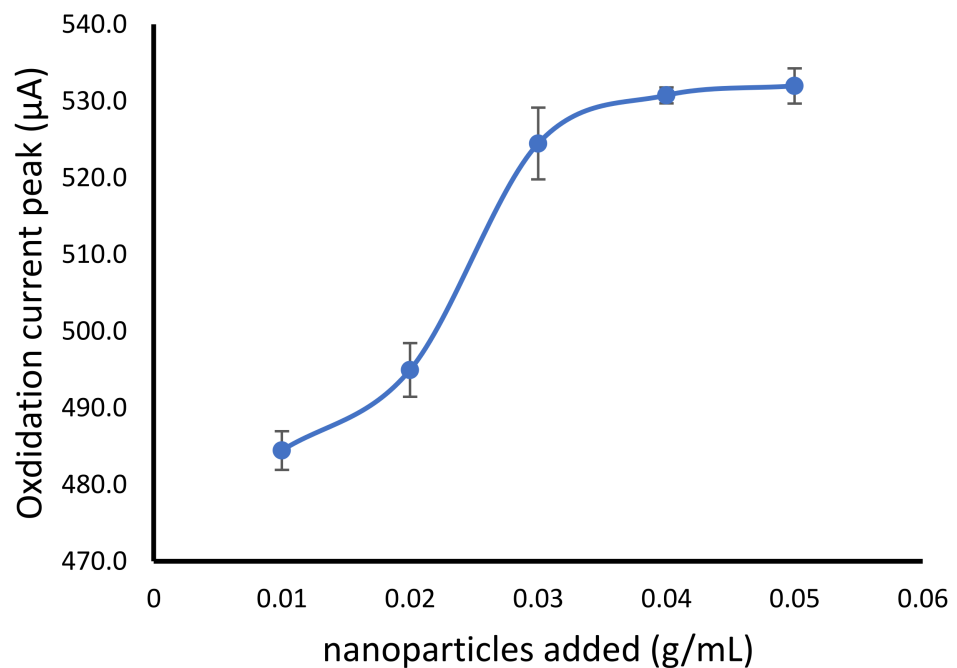


**Figure 3.** Effect of NiFe<sub>2</sub>O<sub>4</sub> nanoparticles addition to alginate cryogel on the increase of oxidation peak of hydrogen peroxide.

### 2.4. Effect of Cyclic Voltammetry Scan Rate

The CV method for the determination of hydrogen peroxide using modified alginate NiFe<sub>2</sub>O<sub>4</sub> nanoparticles has been studied the effect of scan rate using phosphate buffer pH 7.0 with a concentration of 100 mM. The scan rate range used was 0.05–0.13 V/s. The increase in the scan rate causes the increase of electron transfer per second, leading to the accumulation of electrolyte ions. Therefore, each increase in the scan rate would increase the oxidation peak current, making it difficult to obtain the optimum condition of the scan rate, similar to the previous report [33]. However, an increase in scan rate with the increase in the oxidation peak current from 0.06 to 0.11 V/s showed a higher current increase, while the higher scan rate of more than 0.11 V/s showed a lower increase in the oxidation peak current (Figure 4).

### 2.5. Effect of Buffer pH and Concentration on the Detection of Hydrogen Peroxide

The buffer pH was optimized using 0.1 M phosphate buffer with various pH of 6.0, 6.5, 7.0, 7.5 and 8.0. The result showed that the optimum pH for the determination of hydrogen peroxide was at a pH of 7.0 (Figure 5). The increase of buffer pH from 6.0 to 7.0 showed an increase of oxidation current peak. However, the higher pH of more than 7.0 did not significantly increase in the current oxidation peak. The pH of 7.0 was also selected based on the glucose oxidase enzyme having an optimum pH of 7.0 when applied as glucose biosensor [7]. In some cases, the change of pH can lead to a change in oxidation or reduction peak [34], which may be favorable to improve the selectivity. In this study, various pH showed similar oxidation peak potential but different their peak height.

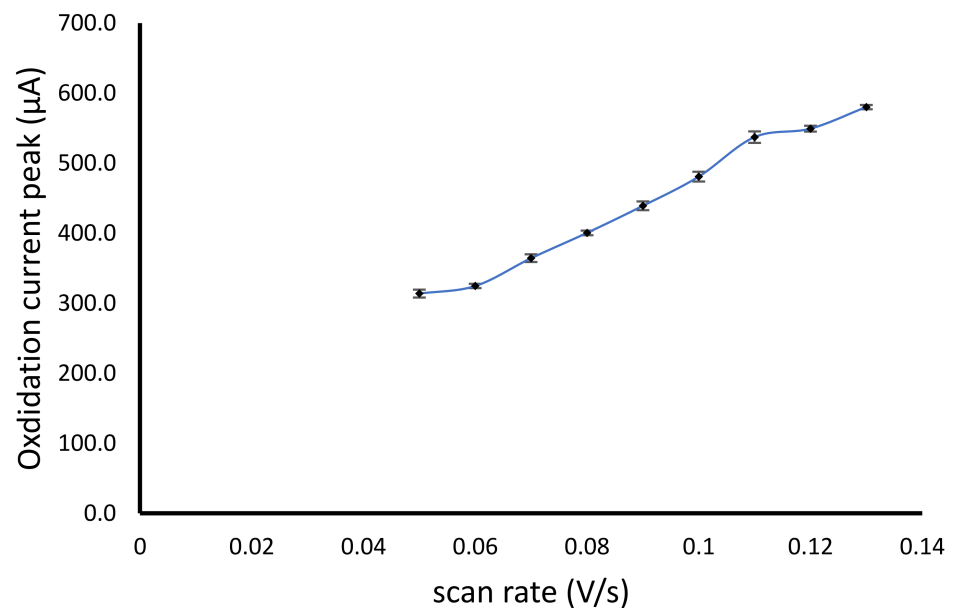


**Figure 4.** Scan rate optimization of the cyclic voltammetry method for hydrogen peroxide determination using modified alginate NiFe<sub>2</sub>O<sub>4</sub> nanoparticles cryogel electrode.

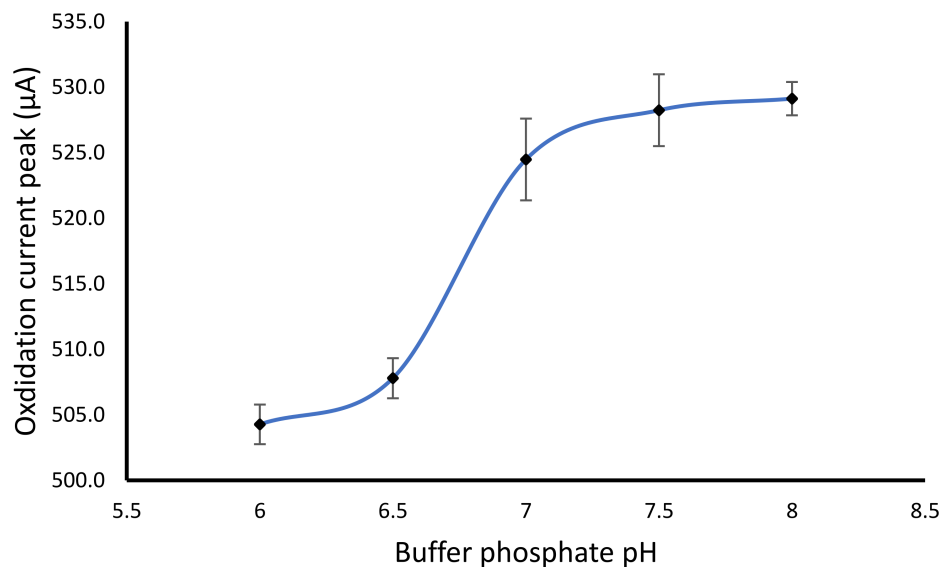


**Figure 5.** Effect of buffer pH on the hydrogen peroxide oxidation peak using the modified alginate-NiFe<sub>2</sub>O<sub>4</sub> nanoparticles cryogel electrode.

The concentration of the phosphate buffer influences the redox behavior of hydrogen peroxide, since the electron transfer highly depends on the electrolyte concentration in the

medium. The result showed an increase in the buffer concentration from 50 to 150 mM, while the higher buffer concentration did not show a significant increase (Figure 6). The buffer concentration of the buffer was an important factor affecting the sensitivity of the biosensor. The concentration of the buffer causes a change in the capacity of the ionic form of the substance in the solution. The higher the buffer concentration, the more free ions from the buffer salt contained in the solution, thus increasing the current value. Optimal buffer concentration could provide a high sensitivity of the biosensor.

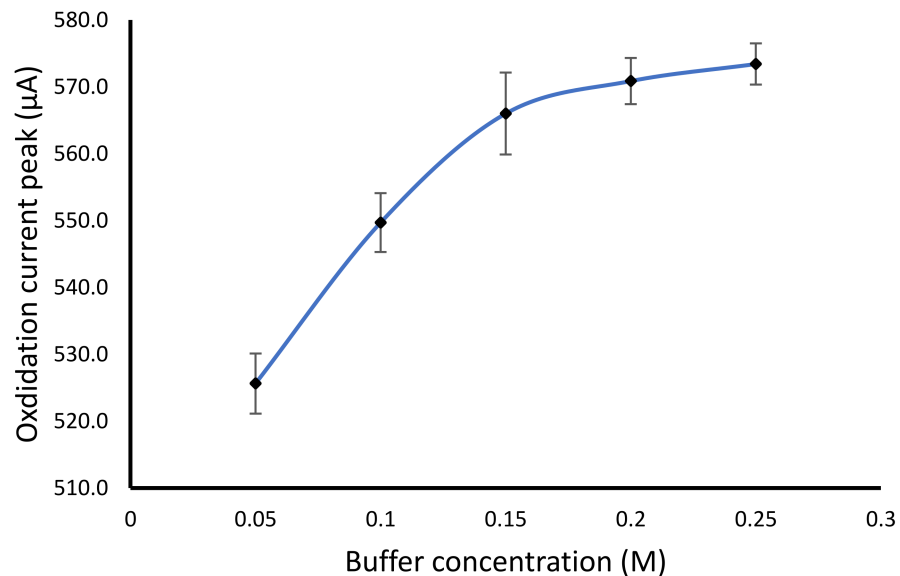
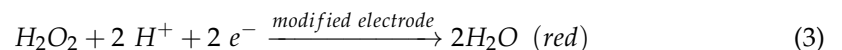
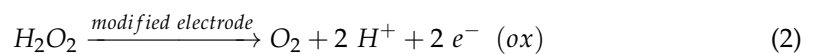
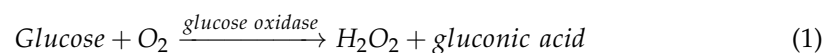


**Figure 6.** Buffer concentration effect on the hydrogen peroxide determination using the modified electrode.

### 2.6. Glucose Determination Using Fabricated Biosensor

The glucose determination was performed with the glucose oxidase enzyme entrapped in the alginate NiFe<sub>2</sub>O<sub>4</sub> nanoparticles cryogel. The electrochemical measurement was based on the determination hydrogen peroxide which results from the enzymatic reaction of glucose catalyzed by glucose oxidase in the following redox reaction:



The result showed that the peaks current was increased linearly with the glucose concentration with the regression equation of  $y = 16.18x + 455.28$  and  $R^2$  of 0.981 (Figure 7). The calculated limit of detection and limit of quantification were 0.32 mM and 1.06 mM respectively. The fabricated electrochemical alginate-NiFe<sub>2</sub>O<sub>4</sub> nanoparticles cryogel based glucose biosensor was more sensitive compared to colorimetric alginate-based glucose biosensor [13] and near-infrared alginate-based glucose biosensor [35].

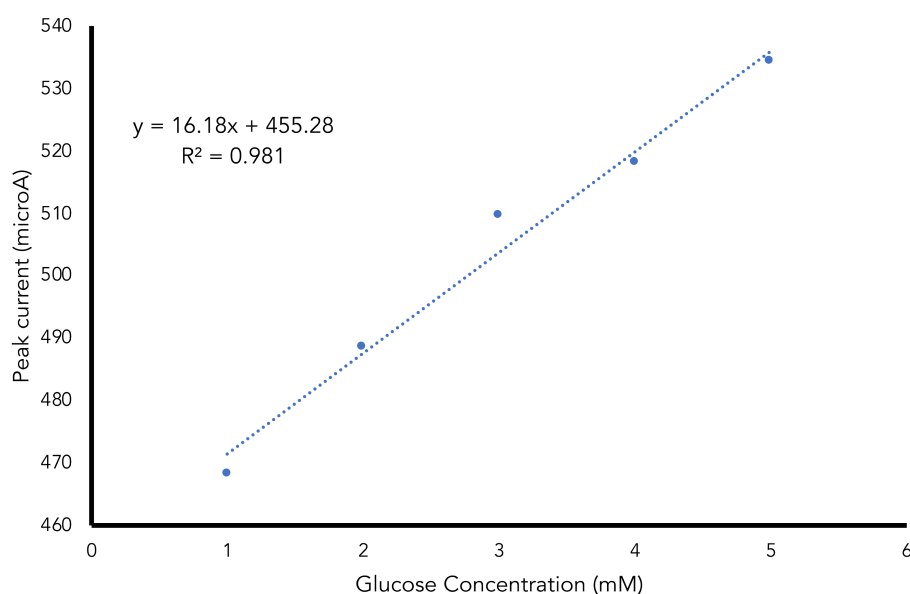


**Figure 7.** Glucose determination using fabricated alginate NiFe<sub>2</sub>O<sub>4</sub> nanoparticles cryogel biosensor.

### 3. Conclusions

Alginate NiFe<sub>2</sub>O<sub>4</sub> nanoparticles composite as supporting material in the fabricated glucose biosensor showed a high surface area and good electron transfer using an electrochemical detector. The optimal conditions obtained were the addition of NiFe<sub>2</sub>O<sub>4</sub> nanoparticles of 0.03 g/mL sodium alginate solution, a scan rate of 0.11 V/s, phosphate buffer pH of 7.0 and buffer concentration of 150 mM. The determination of the glucose using immobilized GOD enzyme showed a linear response with regression equation of  $y = 16.18x + 455.28$  and  $R^2$  of 0.98. The limit of detection obtained was 0.32 and the limit of quantification was 1.06 mM.

### 4. Materials and Methods

#### 4.1. Materials

Alginic acid sodium salt from brown algae (BioReagent, Sigma-Aldrich, St. Louis, MI, USA), glucose oxidase from *Aspergillus niger* (type II,  $\geq 15,000$  U/g solid, Sigma-Aldrich, St. Louis, MI, USA), nickel(II) chloride (NiCl<sub>2</sub>·6H<sub>2</sub>O) Merck KGaA, Darmstadt, Germany), iron(III) chloride (FeCl<sub>3</sub>·6H<sub>2</sub>O) (Merck KGaA, Darmstadt, Germany), glucose anhydrous ( $\geq 98.0\%$ ) (Sigma), acetic acid (CH<sub>3</sub>COOH) (Merck KGaA, Darmstadt, Germany), hydrogen peroxide (H<sub>2</sub>O<sub>2</sub>) 30% (Merck KGaA, Darmstadt, Germany), sodium hydroxide (NaOH) (Merck KGaA, Darmstadt, Germany), disodium hydrogen phosphate (Merck KGaA, Darmstadt, Germany) and sodium dihydrogen phosphate (Merck KGaA, Darmstadt, Germany).

#### 4.2. Apparatus and Measurements

Scanning electron microscopy (SEM) (JSM-6510 LA, JEOL, Tokyo, Japan), operating at 15 kV, was used to examine the morphology of the alginate nanoparticle cryogel. The electrochemical analysis was performed using a three-electrode system with a glassy carbon electrode as a working electrode and Ag/AgCl as a reference electrode and platinum wire as a counter electrode. The electrochemical measurements were carried out using Rodeostat Potentiostat (IORodeo Smart Lab Technology, Pasadena, CA, USA).

#### 4.3. NiFe<sub>2</sub>O<sub>4</sub> Nanoparticles Preparation

Nickel ferrite nanoparticles have been synthesized using the co-precipitation method [36] with NiCl<sub>2</sub>·6H<sub>2</sub>O and FeCl<sub>3</sub>·6H<sub>2</sub>O as ion providers Ni<sup>2+</sup> and Fe<sup>3+</sup>. The mole fraction ratio used was 1:2, by dissolving 1.188 g of NiCl<sub>2</sub>·6H<sub>2</sub>O in 20 mL distilled water and 2701 g of FeCl<sub>3</sub>·6H<sub>2</sub>O in 20 mL of distilled water in a separate glass beaker. The two

solutions were then mixed homogeneously. The mixture of Ni and Fe was then dropwise slowly in the precipitation agent of NaOH under stirring (1000 rpm) at 85 °C for 60 min. The variation of NaOH concentrations used were 3, 5, 7, 9 and 11 M. The resulting nanoparticles were then precipitated continued by washing distilled water for approximately seven times of 50 mL. The precipitated nanoparticles obtained were dried at 90 °C. The brown nanoparticles powder was then used for further procedures.

#### 4.4. Alginate Cryogel Electrode Preparation

Sodium alginate solution was prepared by dissolving 2.0 g of alginate in phosphate buffer (100 mM, pH 7) to get 100 mL of solution. The 50 µL of alginate solution was then drop on the glassy carbon working electrode (3 mm diameter). The electrode with alginate cover was immerse in 2 M CaCl<sub>2</sub> solution and allowed for 30 min to make the crosslink layer of Ca-alginate on the electrode. The electrode was then kept in the freezer at −20 °C for 12 h to continue the crosslinking reaction with the freezing condition for cryogel forming.

Alginate NiFe<sub>2</sub>O<sub>4</sub> nanoparticles were prepared using similar procedure above with the addition of NiFe<sub>2</sub>O<sub>4</sub> to the alginate solution with the concentration of 0.1, 0.2, 0.3, 0.4 and 0.5 g per 100 mL alginate solution. The mixture was then dropped in on the glassy carbon electrode and further the procedure of alginate cryogel modified electrode. The modified electrode with alginate cryogel and alginate NiFe<sub>2</sub>O<sub>4</sub> has been tested using K<sub>3</sub>[Fe(CN)<sub>6</sub>] and H<sub>2</sub>O<sub>2</sub> (in 100mM phosphate buffer, pH of 7.0) solution by cyclic voltammetry method.

#### 4.5. Cyclic Voltammetry Optimization

The optimal condition of the electrochemical cell using cyclic voltammetry (−1.0 to 1.0 V, 3 scans) were performed by varying the scan rate of 0.05, 0.06, 0.07, 0.08, 0.09, 0.10, 0.11, 0.12 and 0.13 mV/s. The solution used was H<sub>2</sub>O<sub>2</sub> 5 mM in phosphate buffer pH 7.0. The best scan rate with the minimum background current was then selected for further study.

#### 4.6. Buffer pH and Concentration Optimization

The buffer pH and concentration were optimized in the H<sub>2</sub>O<sub>2</sub> determination with a variation of pH 6.0 to 8.0 with the various concentrations of 50, 100, 150, 200 and 250 mM. The cyclic voltammetry conditions included the optimized parameters obtained.

#### 4.7. Glucose Determination Using Modified Electrode

Glucose oxidase as biological sensing element was prepared in buffer solution (pH 7.0, concentration 50 mM). The enzyme was immobilized in the working electrode by entrapping method. The glucose oxidase solution was then added to the alginate solution (20 µL/1000 µL) with the total enzyme activity of 50 U per modified electrode made of 50 µL solution of alginate-NiFe<sub>2</sub>O<sub>4</sub> nanoparticles. The mixture was then dropped on the working electrode surface, dipped in the crosslinking agent and kept in the freezer for cryogelation. The modified electrode was then tested to detect glucose standard solution under the optimal condition. Linearity, the limit of detection and limit of quantification were then calculated from the series concentration of glucose determined.

**Author Contributions:** Conceptualization, A.F. and M.D.A.; methodology, A.W. and Z.; validation, D.H., A.F. and H.D.; formal analysis, M.D.A. and Z.; investigation, A.W. and Z.; resources, H.D.; data curation, D.H.; writing—original draft preparation, A.F.; writing—review and editing, M.D.A. and D.H.; visualization, A.F.; supervision, A.F. and D.H.; project administration, Z. and H.D.; funding acquisition, A.F. All authors have read and agreed to the published version of the manuscript.

**Funding:** This research was funded by Universitas Jenderal Soedirman grant number T/591/UN23.18/PT.01.03/2021.

**Institutional Review Board Statement:** Not applicable.

**Informed Consent Statement:** Not applicable.

**Data Availability Statement:** The data presented in this study are available on request from the corresponding author.

**Acknowledgments:** We would like to thank the Universitas Jenderal Soedirman, Indonesia Research Grant of “Riset Unggulan Perguruan Tinggi”.

**Conflicts of Interest:** The authors declare no conflict of interest.

## References

1. Roglic, G. WHO Global report on diabetes: A summary. *Int. J. Noncommun. Dis.* **2016**, *1*, 3. [CrossRef]
2. International Diabetes Federation. *IDF Diabetes Atlas*, 8th ed.; International Diabetes Federation: Brussels, Belgium, 2017; ISBN 9782930229874.
3. Yoo, E.H.; Lee, S.Y. Glucose biosensors: An overview of use in clinical practice. *Sensors* **2010**, *10*, 4558–4576. [CrossRef]
4. Naresh, V.; Lee, N. A Review on Biosensors and Recent Development of Nanostructured Materials-Enabled Biosensors. *Sensors* **2021**, *21*, 1109. [CrossRef]
5. Sohrabi, H.; Hemmati, A.; Majidi, M.R.; Eyvazi, S.; Jahanban-Esfahlan, A.; Baradaran, B.; Adlpour-Azar, R.; Mokhtarzadeh, A.; de la Guardia, M. Recent advances on portable sensing and biosensing assays applied for detection of main chemical and biological pollutant agents in water samples: A critical review. *TrAC Trends Anal. Chem.* **2021**, *143*, 116344. [CrossRef]
6. Fatoni, A.; Anggraeni, M.D.; Dwiasi, D.W. Easy and Low-cost Chitosan Cryogel-based Colorimetric Biosensor for Detection of Glucose. *J. Anal. Chem.* **2019**, *74*, 933–939. [CrossRef]
7. Fatoni, A.; Numnuam, A.; Kanatharana, P.; Limbut, W.; Thammakhet, C.; Thavarungkul, P. A highly stable oxygen-independent glucose biosensor based on a chitosan-albumin cryogel incorporated with carbon nanotubes and ferrocene. *Sens. Actuators B Chem.* **2013**, *185*, 725–734. [CrossRef]
8. Fatoni, A.; Numnuam, A.; Kanatharana, P.; Limbut, W.; Thavarungkul, P. A Conductive Porous Structured Chitosan-grafted Polyaniline Cryogel for use as a Sialic Acid Biosensor. *Electrochim. Acta* **2014**, *130*, 296–304. [CrossRef]
9. Varaprasad, K.; Jayaramudu, T.; Kanikireddy, V.; Toro, C.; Sadiku, E.R. Alginate-based composite materials for wound dressing application: A mini review. *Carbohydr. Polym.* **2020**, *236*, 116025. [CrossRef] [PubMed]
10. Bidarra, S.J.; Barrias, C.C.; Granja, P.L. Injectable alginate hydrogels for cell delivery in tissue engineering. *Acta Biomater.* **2014**, *10*, 1646–1662. [CrossRef]
11. Jain, D.; Bar-Shalom, D. Alginate drug delivery systems: Application in context of pharmaceutical and biomedical research. *Drug Dev. Ind. Pharm.* **2014**, *40*, 1576–1584. [CrossRef]
12. Zufahair, D.R.; Kartika, D.; Kurniasih, M.; Nofiani, R.; Fatoni, A. Improved reuse and affinity of enzyme using immobilized amylase on alginate matrix. *J. Phys. Conf. Ser.* **2020**, *1494*, 12028. [CrossRef]
13. Fatoni, A.; Dwiasi, D.W.; Hermawan, D. Alginate cryogel based glucose biosensor. In Proceedings of the IOP Conference Series, Materials Science and Engineering, Solo, Indonesia, 8–9 September 2015; Volume 107, p. 012010. [CrossRef]
14. Guastaferrero, M.; Reverchon, E.; Baldino, L. Agarose, Alginate and Chitosan Nanostructured Aerogels for Pharmaceutical Applications: A Short Review. *Front. Bioeng. Biotechnol.* **2021**, *9*, 688477. [CrossRef] [PubMed]
15. Gheorghita Puscaselu, R.; Lobiuc, A.; Dimian, M.; Covasa, M. Alginate: From food industry to biomedical applications and management of metabolic disorders. *Polymers* **2020**, *12*, 2417. [CrossRef] [PubMed]
16. Marroquin, J.B.; Rhee, K.Y.; Park, S.J. Chitosan nanocomposite films: Enhanced electrical conductivity, thermal stability, and mechanical properties. *Carbohydr. Polym.* **2013**, *92*, 1783–1791. [CrossRef] [PubMed]
17. Kargan, H. Synthesis of nickel ferrite nanoparticles by co-precipitation chemical method. *Int. J. Phys. Sci.* **2013**, *8*, 854–858.
18. Sagadevan, S.; Chowdhury, Z.Z.; Rafique, R.F. Preparation and characterization of nickel ferrite nanoparticles via co-precipitation method. *Mater. Res.* **2018**, *21*. [CrossRef]
19. Muflihatun, S.S.; Suharyadi, E. Sintesis Nanopartikel Nickel Ferrite ( $\text{NiFe}_2\text{O}_4$ ) dengan Metode Kopresipitasi dan Karakterisasi Sifat Kemagnetannya. *J. Fis. Indones.* **2015**, *19*, 20–25.
20. Bu, Y.; Xu, H.-X.; Li, X.; Xu, W.-J.; Yin, Y.; Dai, H.; Wang, X.; Huang, Z.-J.; Xu, P.-H. A conductive sodium alginate and carboxymethyl chitosan hydrogel doped with polypyrrole for peripheral nerve regeneration. *RSC Adv.* **2018**, *8*, 10806–10817. [CrossRef]
21. Khairy, M.; Gouda, M.E. Electrical and optical properties of nickel ferrite/polyaniline nanocomposite. *J. Adv. Res.* **2015**, *6*, 555–562. [CrossRef]
22. Sadrolhosseini, A.R.; Naseri, M.; Rashid, S.A. Polypyrrole-chitosan/nickel-ferrite nanoparticle composite layer for detecting heavy metal ions using surface plasmon resonance technique. *Opt. Laser Technol.* **2017**, *93*, 216–223. [CrossRef]
23. Unal, B.; Toprak, M.S.; Durmus, Z.; Sözeri, H.; Baykal, A. Synthesis, structural and conductivity characterization of alginic acid- $\text{Fe}_3\text{O}_4$  nanocomposite. *J. Nanopart. Res.* **2010**, *12*, 3039–3048. [CrossRef]
24. Teepoo, S.; Laochai, T. Reusable Optical Biosensor Based on Poly (Vinyl) Alcohol-Chitosan Cryogel with Incorporated Magnetic Nanoparticles for the Determination of Sucrose in Sugar Cane and Sugar. *Anal. Lett.* **2021**, 1–13. [CrossRef]
25. Supramaniam, J.; Adnan, R.; Kaus, N.H.M.; Bushra, R. Magnetic nanocellulose alginate hydrogel beads as potential drug delivery system. *Int. J. Biol. Macromol.* **2018**, *118*, 640–648. [CrossRef] [PubMed]

26. Liu, Z.; Liu, J.; Cui, X.; Wang, X.; Zhang, L.; Tang, P. Recent advances on magnetic sensitive hydrogels in tissue engineering. *Front. Chem.* **2020**, *8*, 124. [[CrossRef](#)]
27. Gila-Vilchez, C.; Bonhome-Espinosa, A.B.; Kuzhir, P.; Zubarev, A.; Duran, J.D.G.; Lopez-Lopez, M.T. Rheology of magnetic alginate hydrogels. *J. Rheol.* **2018**, *62*, 1083–1096. [[CrossRef](#)]
28. Ha, Y.; Ko, S.; Kim, I.; Huang, Y.; Mohanty, K.; Huh, C.; Maynard, J.A. Recent advances incorporating superparamagnetic nanoparticles into immunoassays. *ACS Appl. Nano Mater.* **2018**, *1*, 512–521. [[CrossRef](#)]
29. Kloster, G.A.; Muraca, D.; Londono, O.M.; Pirola, K.R.; Mosiewicki, M.A.; Marcovich, N.E. Alginate based nanocomposites with magnetic properties. *Compos. Part A Appl. Sci. Manuf.* **2020**, *135*, 105936. [[CrossRef](#)]
30. Sharma, S.; Sanpui, P.; Chattopadhyay, A.; Ghosh, S.S. Fabrication of antibacterial silver nanoparticle—Sodium alginate—Chitosan composite films. *Rsc Adv.* **2012**, *2*, 5837–5843. [[CrossRef](#)]
31. Bedê, P.M.; da Silva, M.H.P.; Figueiredo, A.B.-H.d.S.; Finotelli, P.V. Nanostructured magnetic alginate composites for biomedical applications. *Polímeros* **2017**, *27*, 267–272. [[CrossRef](#)]
32. Jie, G.; Kongyin, Z.; Xinxin, Z.; Zhijiang, C.; Min, C.; Tian, C.; Junfu, W. Preparation and characterization of carboxyl multi-walled carbon nanotubes/calcium alginate composite hydrogel nano-filtration membrane. *Mater. Lett.* **2015**, *157*, 112–115. [[CrossRef](#)]
33. Aini, B.N.; Siddiquee, S.; Ampon, K.; Rodrigues, K.F.; Suryani, S. Development of glucose biosensor based on ZnO nanoparticles film and glucose oxidase-immobilized eggshell membrane. *Sens. Bio-Sens. Res.* **2015**, *4*, 46–56. [[CrossRef](#)]
34. Shah, A.H.; Zaid, W.; Shah, A.; Rana, U.A.; Hussain, H.; Ashiq, M.N.; Qureshi, R.; Badshah, A.; Zia, M.A.; Kraatz, H.-B. pH Dependent electrochemical characterization, computational studies and evaluation of thermodynamic, kinetic and analytical parameters of two phenazines. *J. Electrochem. Soc.* **2014**, *162*, H115. [[CrossRef](#)]
35. Chaudhary, A.; Harma, H.; Hanninen, P.; McShane, M.J.; Srivastava, R. Glucose response of near-infrared alginate-based microsphere sensors under dynamic reversible conditions. *Diabetes Technol. Ther.* **2011**, *13*, 827–835. [[CrossRef](#)] [[PubMed](#)]
36. Vigneswari, T.; Raji, P. Structural and magnetic properties of calcium doped nickel ferrite nanoparticles by co-precipitation method. *J. Mol. Struct.* **2017**, *1127*, 515–521. [[CrossRef](#)]